

de Haas-van Alphen Effect in Dilute Alloys of Bismuth in Lead*

J. R. ANDERSON AND D. C. HINES†

Department of Physics and Astronomy, University of Maryland, College Park, Maryland 20742

(Received 27 July 1970)

An *in situ* NMR technique has been used to make accurate (~ 2 parts in 10^4) measurements of several de Haas-van Alphen frequencies in pure lead for two of the primary symmetry directions, $[100]$ and $[110]$. By the same method the variation of the $[100]$ β frequency with the addition of up to 0.2% bismuth has been investigated. The alloy results identify the β oscillations as being due to an electronlike piece of Fermi surface. At small impurity concentrations, the dependence of the frequency on concentration is in good agreement with the rigid-band model. However, at the higher concentrations there is a tendency for the frequency changes to be smaller than predicted by the rigid-band model and we interpret this trend to be due to an increase in the density of states, indicating that electrons are beginning to fill the fourth zone. It is not clear from our results whether the fourth zone begins above or below the pure-lead Fermi energy, but taken at face value, our measurements would suggest that it begins about 4 meV above the Fermi energy.

INTRODUCTION

There has been considerable interest in the electronic structure of metallic alloys since the Hume-Rothery rules¹ indicated that the electron-per-atom ratio was an important parameter in determining alloy phase boundaries. This interest has been enhanced in recent years by advances in the experimental techniques of studying the Fermi surface and by increased knowledge of the Fermi surfaces of pure metals. For the de Haas-van Alphen (dHvA) effect, improvements in the signal-to-noise ratio and in magnetic field measurements have been particularly important. The exponential dependence of the amplitude on scattering means that doping by even a few tenths of 1% of impurity can reduce the amplitude by at least an order of magnitude. In addition, accurate field measurements are necessary in order to detect the small changes in dHvA frequencies that result from the addition of small amounts of impurity.

Few dHvA experiments have been performed on polyvalent metal alloys because the changes in dimensions of the large pieces of Fermi surface are quite small for the low concentrations of impurity at which measurements can be performed. However, aluminum alloys were studied in some detail by Shepherd and Gordon,² and some early exploratory measurements were made on lead alloys by Gold.³ In addition, zinc alloys have been investigated by Higgins and Marcus,⁴ although the results are complicated here by changes in the c/a ratio on alloying.

The Fermi surface of pure lead has been investigated in detail by Anderson and Gold⁵ (hereafter referred to as AG) using the dHvA effect. Their results are in qualitative agreement with a nearly free-electron Fermi surface consisting of a large second-zone hole surface and a multiply connected third-zone electron surface of $[110]$ arms. The third-zone Fermi surface is shown schematically in Fig. 1.

There is an ambiguity in the interpretation of the AG results, however, which can be cleared up by the alloy studies. The β oscillations, which have been

identified with the junction of the third-zone arms (the ν orbit in Fig. 1) could also be assigned to the "doughnut hole" in the (100) face (the ξ orbit). In the former case the orbit is electronlike, and in the latter holelike. Pressure studies in lead⁶ have shown the effect of changing the lattice parameter on the Fermi surface. This procedure is somewhat complementary to that of alloying, for which the lattice parameter remains essentially fixed, but the Fermi level is changed. Although the pressure results support the assignment of the β oscillations to electron orbits, the possibility remains that this interpretation is incorrect. For the alloys there is less ambiguity, and one expects an electronlike orbit to increase in size with the addition of a donor impurity such as bismuth, and a holelike orbit to decrease.

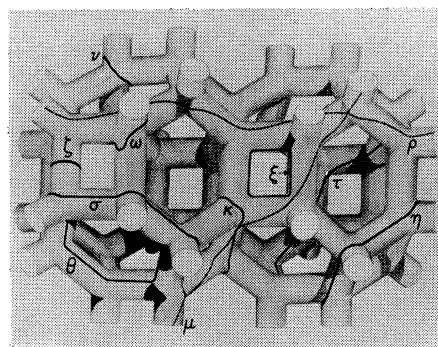


FIG. 1. Third-zone Fermi surface of lead (schematic).

In the present investigation, we have observed dHvA oscillations in pure lead for several crystallographic orientations and have studied oscillations in lead alloys doped with up to 0.2% bismuth. We have also obtained values for the Dingle temperature in these alloys as a measure of electron scattering. Since the relative frequency changes for these oscillations are of the same order as the impurity concentrations, an *in situ* nuclear-magnetic-resonance (NMR) technique was developed which allowed us to make absolute

frequency determinations with sufficient accuracy to observe these small changes.

In order to discuss experimental results, we shall refer to the standard dHvA expressions given below. In a detailed analysis, Lifshitz and Kosevich⁷ showed that the oscillating part of the magnetization is given by

$$M = \sum_{n=1}^{\infty} C_n e^{-n\lambda\mu X/H} T H^{-1/2} \sin\left(\frac{2\pi F n}{H} + \phi_n\right) \times \left(\sinh \frac{n\lambda\mu T}{H}\right)^{-1}, \quad (1)$$

where C_n is an amplitude factor which depends on the particular orbit being observed,

$$\lambda = 2\pi^2 m c k / e \hbar = 147 \text{ kOe/deg}, \quad (2)$$

μ is the cyclotron mass ratio, defined by

$$\mu = (\hbar^2 / 2\pi m) (\partial \mathcal{Q}_0 / \partial E), \quad (3)$$

and ϕ_n is a phase factor. The exponential term, obtained by Dingle⁸ and Brailsford,⁹ contains the Dingle temperature X , given by

$$X = \hbar / 2\pi k \tau, \quad (4)$$

where τ is the lifetime of a state at the Fermi energy. The dHvA frequency is

$$F = \hbar c \mathcal{Q}_0 / 2\pi e, \quad (5)$$

where \mathcal{Q}_0 is the extremal cross-sectional area of the Fermi surface in a plane normal to the direction of the magnetic field.

THEORY

A. Rigid-Band Model

For the interpretation of our measurements we have made the following assumptions: (a) The alloys are substitutional—that is, the impurity atoms occupy host-lattice sites and are not interstitial; (b) the alloys are disordered; the positions of impurity atoms are not correlated; (c) they are dilute; and (d) there is no change in the host-lattice parameter a . The first three assumptions are important for comparison with the rigid-band theory. The last is justified on the basis of pressure dHvA studies on lead⁶ coupled with measurements of lattice parameter versus bismuth concentration¹⁰ which show that the effects of lattice-parameter changes on the Fermi surface are an order of magnitude smaller than the expected variations due to alloying.

Perhaps the simplest approach to the effects of alloying on the electronic properties of metals is to assume that nothing happens except that the number of electrons in the bands is changed by the differences in valence between the solvent and the solute metals; the result is a shift in the Fermi energy. This is the

rigid-band model (RBM), which can be described mathematically in the following way. Consider a metal with N conduction electrons per atom. If a fraction C of those atoms is replaced by atoms with $N+Z$ electrons per atom, the metal now has an average of $N+CZ$ electrons per atom. Expanding the energy about the Fermi energy, one finds, to second order, that the Fermi-energy shift ΔE is

$$\Delta E = [\Delta N / n_0(E_F)] - [(\Delta N)^2 / 2n_0(E_F)^3] [\partial n_0(E_F) / \partial E], \quad (6)$$

where $n_0(E_F)$ is the density of states at the Fermi energy of the pure metal. Since ΔN is just ZC , the first-order change in the Fermi energy is

$$\Delta E = ZC / n_0(E_F). \quad (7)$$

Following Heine,¹¹ we define a parameter R such that

$$R = (\Delta \mathcal{Q} / \mathcal{Q} Z C) = \pm (mc / \hbar e) (\mu \Delta E / F Z C), \quad (8)$$

where $\Delta \mathcal{Q}$ is the change in extremal cross section of the Fermi surface, and F is the dHvA frequency corresponding to area \mathcal{Q} . Here ΔA and ΔE are assumed to be small and are related by Eq. (3). The sign is positive for an electron band, and negative for a hole band. We can make the rigid-band assumption by setting $\Delta E = CZ / n_0(E_F)$, and then

$$R = \pm (mc / \hbar e) [\mu / F n_0(E_F)]. \quad (9)$$

It is expected that if the RBM holds and the density of states is constant over the concentration range of interest, R will be constant. Variations in R can be taken to indicate a failure of the RBM or a change in the density of states from the second-order term of Eq. (6) (or perhaps both).

An apparent fallacy in the RBM was pointed out by Mott,¹² who argued that because of screening, the electronic density, and hence the Fermi energy, would be unchanged some distance from the impurity. This second point of view was reconciled with the RBM by Friedel,¹³ who showed by means of a perturbation argument that although the impurity atoms are screened and the Fermi energy is unaltered, all the energy levels in the band are shifted. To first order, this shift is just that required, so that the change in energy between the bottom of the band and the Fermi energy is the same as obtained in the RBM. It should be noted that it has been shown by Brailsford⁹ that the RBM result is valid even if the energy-level shift is a function of energy.

B. Density of States and Effective Mass

The parameter R of Eq. (9), which is a measure of the changes in Fermi-surface (FS) dimensions on alloying, contains both the density of states and the cyclotron mass. Values of these quantities obtained

from band-structure calculations which fit the FS information differ from values derived from experimental results (i.e., cyclotron resonance, specific heat, etc.). These differences are believed to be due to enhancement of the band-structure values by many-body effects not included in the computations. As a result, some question has arisen in the literature^{2,14} as to which values ought to be used in equations such as (9). To be consistent, one ought to use calculated values for both quantities or measured values for both. Furthermore, since the density of states and the mass are related by

$$n_0(E_F) = \frac{m}{2\pi^2\hbar^2} \int_{\text{FS}} \mu(k_z) dk_z, \quad (10)$$

one would expect them to be affected in much the same way by enhancement. Direct evidence that they are affected similarly is provided by the work of AG in lead and O'Sullivan *et al.*¹⁵ in copper, silver, and gold. They obtain the result that the ratio $\mu/n_0(E_F)$ is nearly the same for calculated as it is for measured values in these metals.

The point here is that the authors cited above^{2,14} have used a band-calculation density of states and have then placed some significance on the fact that their results were best fitted by using a band-calculated mass rather than a measured one. On the basis of the above discussion, it is our belief that this result is to be expected and provides no additional physical insight.

Several experiments indicate that the RBM is applicable to the polyvalent metals. For example, Shepherd and Gordon² prepared alloys of aluminum containing Ag, Mg, Zn, Si, and Ge and an isoelectronic alloy containing Zn and Ge. They found excellent agreement with RBM predictions in all cases, which included concentrations up to 1%. Furthermore, they observed an excellent correlation between measured Dingle temperatures and impurity concentration. Of special interest was the isoelectronic alloy AlZnGe, which contained 0.1% each of Zn and Ge, and which showed no significant difference in FS dimensions from pure Al.

In lead alloys, the only dHvA work has been the preliminary investigation by Gold,³ which may not be even qualitatively correct. However, determinations have been made of the electronic specific-heat coefficient γ from the superconducting critical field curve; this γ is proportional to the electronic density of states at the FS and therefore should reflect changes in the density of states upon alloying. In an early study, Pech¹⁶ obtained a change in γ of about 15% for an isoelectronic alloy of Pb containing 1% of both Bi and Tl, compared with a 60% change for a 1% alloy of only Bi. A later, more careful, investigation by Chol¹⁷ determined the changes in γ for a similar isoelectronic alloy to be less than 1%, while the change

in γ for a 1% Bi alloy was 32%. We take these results to indicate that the density of states, and hence the band structure of Pb, is virtually unchanged by alloying with Bi and Tl to these concentrations, so that the RBM should be applicable.

In order to go beyond the RBM it is tempting to follow Friedel¹³ and Heine¹¹ and use the Thomas-Fermi model to obtain higher-order corrections for the effects of screening. However, the Thomas-Fermi model is probably not the correct approach to use here. As Cutler¹⁸ has pointed out, the Thomas-Fermi model tends to overestimate the electron concentration near the ion, because it does not take into account the repulsion due to orthogonalization to the core states. This is partially canceled in the linear approximation (equivalent to the RBM) by the fact that it underestimates the screening effects of these electrons. However, the primary effect of the inclusion of higher-order terms is to increase even more the electron concentration near the cores. Thus at the present time there seems to be no satisfactory extension improving upon the RBM.

EXPERIMENT

The magnetic field was produced by a 55-kOe Westinghouse superconducting magnet. The field was swept by operating the magnet power supply in the constant-voltage mode and sensing the induced voltage across the magnet, $L di/dt$ as the voltage to be held fixed. This produced a magnet current sweep rate essentially constant in time.¹⁹ The sensed voltage was nulled against a variable external reference, allowing the rate to be varied as desired.

The sample magnetization was measured by a low-frequency modification of the field-modulation technique first developed by Shoenberg and Stiles.²⁰ The details of this method are described by Stark *et al.*,²¹ and the actual apparatus used in this experiment is described by Hines.²²

The magnetic field was measured by an NMR probe located adjacent to the center of the dHvA sample. The probe, labeled B in Fig. 2, consisted of two series-connected coils of nine turns each, filled with finely ground aluminum powder. The marginal oscillator used for the NMR measurements was essentially that of Hill and Hwang,²³ and we were able to obtain continuous variation of the frequency from about 25 to 60 MHz with the Al²⁷ resonance (1.1112 MHz/kOe including the Knight shift²⁴). We could therefore use a field sweep range from about 23 to 55 kOe. The modulation field for the dHvA measurements was also suitable for the NMR (~ 10 -Oe peak), so that both kinds of measurements could be performed simultaneously. The audio output of the marginal oscillator was differentiated by a lock-in amplifier to increase the signal-to-noise ratio and to allow more accurate determination of the resonance

center. When the center of the resonance was observed, a mark was made on the dHvA oscillation recording, and the frequency of the oscillator was noted. In this manner the center of the resonance could be determined to within 1 Oe.

The data for the dHvA frequency measurement consisted of an NMR frequency associated with a calibration mark on the chart recording of the oscillations. The frequency was obtained by plotting the cycle number corresponding to each calibration mark (to the nearest tenth of a cycle measured from an arbitrary origin) against the inverse field associated with the same mark. (Approximately 1000 cycles were counted for each measurement.) The magnitude of the slope of the resulting straight line was the frequency. The slope was determined by standard least-squares fitting techniques with a computer program which also computed the standard estimate of error of the slope.

The Dingle temperature was obtained from measurements of the variation of the dHvA amplitude as a function of magnetic field. The relationship by which the Dingle temperature is obtained is

$$-\frac{\lambda\mu X}{H_0} = \ln \left(\frac{C_n \sinh(\lambda\mu T/H_0) H_0^{1/2}}{J_\nu(\alpha)} \right) \quad (11)$$

[see Eq. (1) and Ref. 22], where H_0 is the applied quasistatic field, $J_\nu(\alpha)$ is a ν th-order Bessel function of the first kind with argument α ($=2\pi F h_m H_0^{-2}$), and h_m is the modulation field amplitude. A plot of the right-hand side versus $-\lambda\mu/H_0$ yields a straight line of slope X , which may also be analyzed by the least-squares technique.

SAMPLE PREPARATION

The starting material for all the samples was 99.9999%-pure lead from Cominco American, Inc. All the crystals were pulled from a melt to minimize the dislocation density. In order to minimize handling damage, the pulled crystals were cut into individual samples by the floating acid technique²⁵ whereby a layer of acid is floated on a heavier, inert liquid, into which the crystal is lowered until the desired length extends below the acid layer. The acid cuts through the crystal, and the separated sample sinks gently

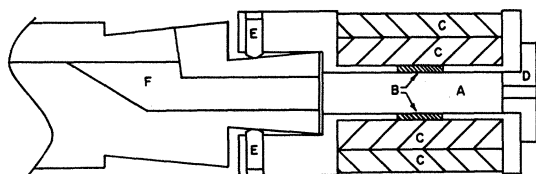


FIG. 2. Cutaway drawing of the pickup coil. A, sample space; B, NMR probe coils (flat pancake coils); C, counterwound pickup coils; D, delrin plug; E, fine orientation adjustment screws; F, access hole for NMR coaxial cable.

TABLE I. dHvA frequencies in lead.

Oscillation orientation	Sample	Frequency (10^8 G)	Area $[(2\pi/a)^2]^a$
$\alpha[100]$	10A5	2.0436 ± 0.0002	1.1864
$\beta[100]$	10B3	0.51245 ± 0.00002	0.29752
$\beta[100]$	10B5	0.51255 ± 0.00007	0.29761
$\beta'[100]^b$	10B3	0.5338 ± 0.0001	0.2980 ₆
$\alpha[110]$	10D1	1.5911 ± 0.0005	0.9238
$\alpha^{(2)}[110]$	10D1	3.1815 ± 0.0003	
$\alpha + \gamma[110]^b$	10D1	1.7722 ± 0.0005	
$\gamma[110]^b$	10D1	0.1809 ± 0.0002	0.1053
$\gamma'[110]^b$	10D1	0.1778 ± 0.0002	0.1032

^a a ($=4.90$ Å) is the lattice parameter extrapolated to low temperatures (see Ref. 5).

^b Not measured directly. Determined from analysis of beats.

to the bottom of the beaker. The cutting acid was composed of 50% glacial acetic acid and 50% hydrogen peroxide (C.P. 30%). The heavy base liquid was ethylene dibromide.

Because the samples varied somewhat in diameter, it was necessary to find a sufficiently adaptable way of mounting them in the pickup coil so that different sample sizes could be accommodated without allowing the samples to tilt or move once they had been oriented. It was desirable that no grease or adhesive be used, since differential contraction rates upon cooling to low temperature could cause straining of the samples. The solution reached was to take a drill about the same diameter as the sample and wrap it with Teflon thread-seal tape until the outside diameter was just that of the sample hole in the pickup coil. The drill was removed and the sample inserted. If space still remained around the sample, small strips of the tape could be inserted to fill the gaps. The Teflon was sufficiently springy to hold the sample in place without damage and did not become completely rigid even at helium temperatures. The sample was prevented from falling out of the coil by a delrin plug with a small hole in it to allow helium access (D in Fig. 2).

Because the variations in dHvA frequencies to be measured were so small, it was necessary to ensure that the effect to be observed was not masked by frequency changes due to variations in sample orientation. To assure accurate alignment, the pickup coil was mounted on the sample holder in such a way that small adjustments in orientation could be made after the sample had been mounted. The mechanism for doing this is shown in Fig. 2. The base of the cone-shaped end on the sample holder served as a pivot point. Four screws, labeled E in the figure, equally spaced around the upper end of the pickup coil, allowed two independent degrees of freedom of motion. The sample-holder assembly was mounted in the x-ray machine so that an end-on Laue picture could be taken of the sample through the hold in the bottom

TABLE II. Changes in frequency of β [100] oscillations with alloying.

Sample	Bi concentration (%)		Frequency (10^8 G)	$\Delta F/F_0$ (%)	X ($^{\circ}\text{K}$)
	Nominal	Measured			
10B3	0.0	0.0	0.51245 ± 0.00002	0	0.12 ± 0.06
10A8	0.1	0.058 ± 0.009	0.51278 ± 0.00015	0.064 ± 0.025	0.37 ± 0.09
10A10	0.1	0.074 ± 0.011	0.51311 ± 0.00005	0.130 ± 0.011	0.71 ± 0.15
10B8	0.2	0.135 ± 0.020	0.51345 ± 0.00005	0.194 ± 0.008	0.85 ± 0.12
10B7	0.2	0.150 ± 0.023	0.51366 ± 0.00005	0.236 ± 0.009	1.22 ± 0.09
10B12	0.3	0.215 ± 0.032	0.51385 ± 0.00005	0.270 ± 0.011	1.55 ± 0.13

of the coil. It was thus possible to align the desired axis of the crystal parallel to the sample holder to within $\frac{1}{2}^{\circ}$.

There are a number of chemical and spectroscopic methods by which one can, in principle, make a determination of the absolute impurity concentration, but in practice, at the impurity concentrations ($\sim 0.1\%$) and sample weights (~ 0.2 g) used here, none of them is very accurate. The concentrations of bismuth were considered to be too large for spark source mass spectrometer evaluation, and the total weight of each sample was too small for atomic absorption measurements. (For the latter method about 1 g of sample is required and the analyses are accurate to $\pm 0.5\%$.) Therefore a spectrographic analysis was made of these alloys, which required only 10–20 mg of material and could be made with an estimated accuracy of $\pm 15\%$.

For this analysis, each sample was divided into five roughly equal parts, and the measurements were made independently on the second and fourth sections (i.e., the pieces next to the ends). This approach gave an indication of the variation in concentration along the sample length, as well as leaving the middle section for a future check if that became necessary. An analysis was made for bismuth concentration in each of the five samples. In addition, an analysis of all metallic impurities was carried out on the pure-lead sample 10A10. Except for traces of silver, a residue of the silver paint used in mounting the sample for another experiment, metallic impurities were not detected by the instrument, which has a sensitivity of < 1 ppm. The analyses were performed by Ledoux and Co.,²⁶ and the results are given in the next section.

Perhaps the most reliable measure of relative concentration should be the Dingle temperature. It is a measure of the mean free path of the electrons and should be linear with concentration for dilute alloys. Furthermore, it samples the same region of the alloy as the frequency measurement and should therefore be a more reliable measure of the concentration of interest than a method which determines the average concentration over the entire sample. For this reason we relied heavily on our Dingle-temperature measurements in this study.

RESULTS

In pure lead we have made accurate measurements of the fundamental and second-harmonic dHvA frequencies for the α and β oscillations in the [100] direction and the α oscillations in the [110] direction. (The α oscillations are high-frequency oscillations attributed to the second-zone hole surface.⁵) Some of these results are shown in Table I and indicate the accuracy with which we believe the measurements have been made. The results of AG are not in close agreement with these results, but it has been determined that there was a systematic error in their measurements amounting to several percent, and the present values are in excellent agreement with their corrected values.^{27,28} Additional frequencies which were not measured directly were determined from a detailed analysis of the beat structure in the observed oscillations.

The measured concentrations for the alloy samples are listed in Table II along with the weighed concentrations of the melt from which they were pulled. The errors in the measured values represent the $\pm 15\%$ precision of the measurement estimated by Ledoux and Co. Concentrations were measured on two separate parts of each sample as described in the preceding section, and in the case of sample 10B12 the middle

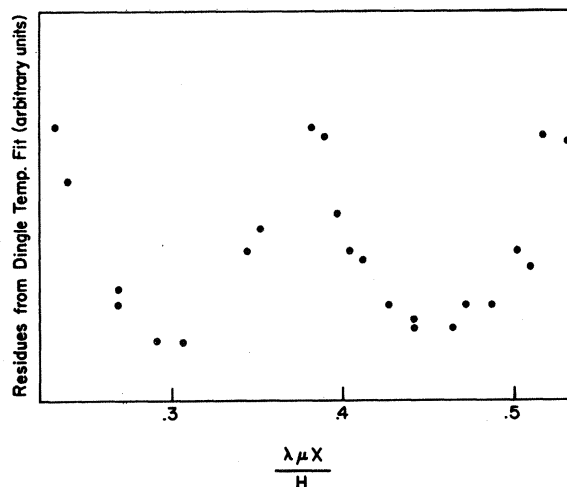


FIG. 3. Residues from Dingle-temperature fit as a function of $(\lambda \mu X / H) \cdot X = 0.075^{\circ}\text{K}$.

portion was analyzed as well. For samples 10B8 and 10B7 there was considerable variation along the length; for 10B8 the two measured values were 0.135 and 0.195%, and for 10B7 they were 0.150 and 0.175%. The lower values were chosen as being the best estimates of the significant concentrations for the following reason: Because of the exponential dependence of the dHvA amplitude on mean free path, our experiment samples only the purest part of the crystal, and we therefore expect that only the smaller value is important.

The results of the frequency measurements for the alloys are given in Table II along with the relative changes in frequency, using the pure sample 10B3 as a reference. This sample was used for the reference because it was oriented slightly better than 10B5 (see Table I). Dingle-temperature measurements on the alloys and on the reference pure sample are also listed in Table II. The effective mass was taken as $\mu=1.20$,²⁵ and was assumed to be unchanged by alloying. The pure-lead value for the Dingle temperature is in good agreement with that obtained by Phillips and Gold,²⁵ and the values increase monotonically with frequency in the alloys.

In most cases the errors quoted for the various measurements are related to the statistical nature of the fitting process used and not to estimates of any systematic errors which might be present. Except in the case of sample 10A8, the frequencies listed in Tables I and II represent the mean of the values obtained for increasing and decreasing fields separately, with weighting by the inverse square of the standard

deviation for each frequency measurement. The inverse-square error is then the sum of the inverse squares of the errors in the individual measurements. This procedure is justified if the values to be averaged come from the same distribution. In our case, we found that the difference in frequency values between increasing and decreasing field sweeps was roughly the same as the standard deviation of the estimate of the frequency. This close agreement allows us to assume the two values are from the same distribution and that hysteresis does not significantly affect the results.

The case of sample 10A8 was different from the others because it was significantly misoriented in the field, and an exact factor to correct for this misorientation could not be determined. The values for 10A8 were arrived at by the following technique. According to the AG model, the γ oscillations are associated with the cross sections of the third-zone arms (orbit ζ in Fig. 1). These cross sections are all the same exactly at $[100]$, but as the field direction moves away from $[100]$, they differ from one another. As a result, beats are observed in the γ oscillations when the field is not in the $[100]$ direction. The cross sections vary most rapidly with respect to one another as one rotates in the (110) plane. The angular variation of frequency for the β oscillations, however, is much smaller than that of the γ 's and is fairly isotropic. One therefore has a measure of the maximum error which could be made in the β frequency due to misorientation by comparing the angular dependence of the β 's with that of the γ 's in the (110) plane. Such a computation was made on the basis of the AG model modified to include nonlocal contributions.²⁷ The variation in the γ oscillations could be measured directly by counting the number of oscillations observed per beat. For all the samples other than 10A8, the maximum correction in the β 's was found to be less than 10^{-4} , corresponding to a maximum misorientation of $< \frac{3}{4}^\circ$, and hence smaller than the statistical uncertainties, but for 10A8 it amounted to 5×10^{-4} (1.5°). Since this value corresponded to the maximum correction, the true β frequency lay somewhere between the measured value and a value corrected by the above factor. Because there was no way of determining exactly where in this range the true value lay, it was chosen to lie halfway between, with the error bars corresponding to the upper and lower limits. From our error analysis we have concluded that the accuracy of the frequency measurements is also well represented by the statistical errors.

The Dingle-temperature values and statistical errors were determined by combining the data for increasing and decreasing field sweeps. Since there are long-period beats in the β oscillations,²⁵ which were not taken into account in the fitting procedure, the quoted errors are not entirely due to random errors in the measurement, but are greatly increased by the sys-

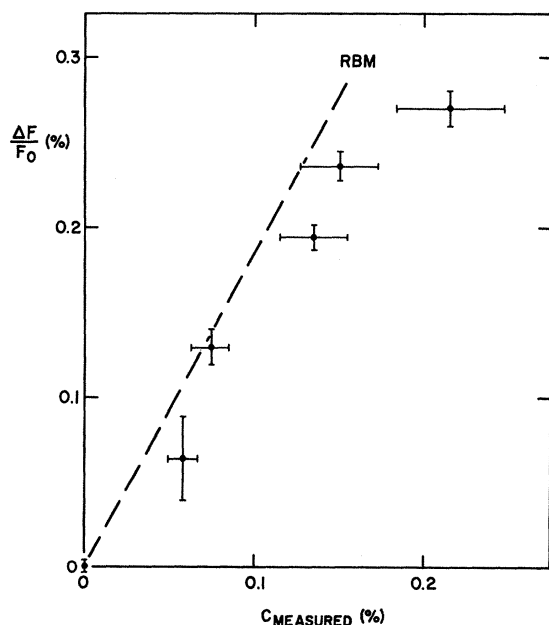


FIG. 4. Relative changes in dHvA frequency as a function of measured bismuth concentration in the samples. The line represents the RBM prediction.

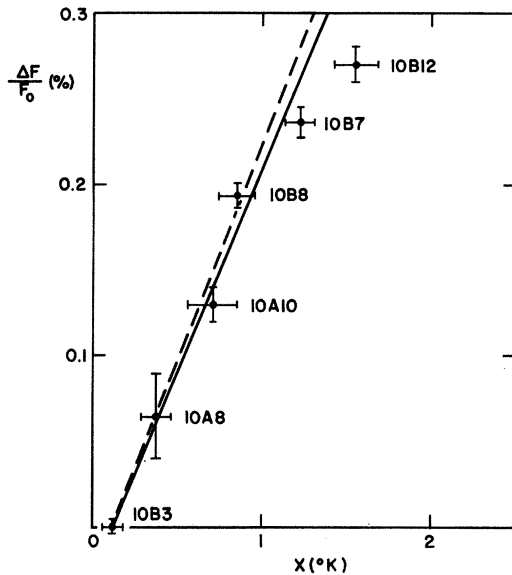


FIG. 5. Relative frequency changes versus Dingle temperature. Solid line is the RBM prediction using measured values of μ and $n_0(E_F)$; dashed line uses the computed values of Anderson *et al.* (Ref. 27).

tematic variation in amplitude due to the beats. In Fig. 3 we show an example of this variation in the residues from the least-squares fit used in determining the Dingle temperature. The period shown corresponds to the beating of about 600 cycles in the β oscillations. No attempt has yet been made to separate the contributions from the two frequencies. The absolute errors in the Dingle-temperature measurements are rather difficult to determine, but because of the excellent agreement of our pure-lead value with that of Phillips and Gold,²⁵ we believe that the accuracy is comparable to the precision.

DISCUSSION

The first, and most obvious, point to note in Table II is that the β oscillation frequencies increase monotonically with increasing bismuth concentration. This is extremely strong evidence that these oscillations correspond to an electronlike piece of FS, and therefore should be assigned to the ν orbit, in agreement with AG.

In Fig. 4 is shown a plot of the relative frequency changes as a function of the measured bismuth concentration. The dashed line represents the RBM prediction from the modified AG model²⁷ of the lead FS. The fit is reasonably good, but would be improved if lower values were taken for the concentrations, consistent with our conclusion that the spectroscopic measurement tends to overestimate the concentration. A similar plot of relative frequency change as a function of Dingle temperature is shown in Fig. 5. It should be noted that there is less scatter in this plot, in line with

our belief that the Dingle temperatures are a more representative indication of the concentrations of interest than are the spectroscopic measurements. This is the figure which we wish to compare with theory. To make the comparison, we must establish the relationship between the concentration and the Dingle temperature. From a least-squares fit we obtain for the relationship between the Dingle temperature X and the concentration C

$$X = 0.09 + 674C. \quad (12)$$

This result leads to the rigid-band prediction indicated by the two lines in Fig. 5, the dashed one obtained from the μ and $n_0(E_F)$ of the modified AG band calculation and the solid one from the value of μ measured by Phillips and Gold²⁵ and of $n_0(E_F)$ determined from the specific-heat measurements of van der Hoeven and Keesom.²⁹ Both fit the data quite well at small concentrations, and there seems to be no way to choose between them. At the larger concentrations there is a definite trend for the points to lie below these lines, indicating either a failure of the RBM or an increase in the density of states near the FS. The significance of that trend is explored in the following paragraph.

Several investigators have determined the specific-heat coefficient γ in lead alloys from measurements of the superconducting critical field and temperature. Sekula and Kernohan³⁰ have measured the changes in the density states with the addition of Tl impurity; Pech¹⁶ has done the same thing for Bi impurity, while Chol¹⁷ has used both types of impurity. Sekula and Kernohan found that, assuming the RBM, the density of states reaches a peak about 0.14 eV below the pure-lead Fermi energy. The position of this peak is in rough agreement with a preliminary nonlocal pseudopotential calculation by Anderson *et al.*,²⁷ which places such a feature about 0.1 eV below the FS. Chol observed a slight drop in the density of states just below the pure-lead FS before the rise observed by Sekula and Kernohan begins (see Fig. 6). The minimum occurs about 1 meV below the FS, and the value of the density of states there is sufficiently

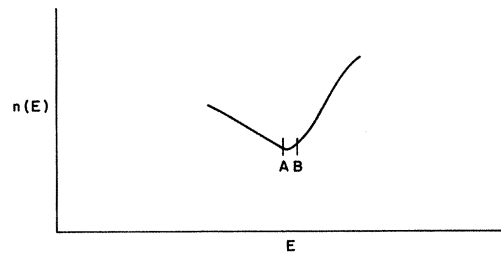


FIG. 6. Lead density of states near the Fermi energy (schematic). The present study indicates that the Fermi energy is located at point A. Chol's result (Ref. 17) indicates that it is at point B.

close to the pure-lead value that the significance of the drop is questionable. Both Pech and Chol observed a sharp rise in the density of states above the Fermi energy, corresponding, most probably, to the incipience of the fourth zone (see Fig. 6). It is this feature which we believe is responsible for the apparent increase in the density of states indicated by the tendency of our data to fall below the RBM prediction at higher bismuth concentrations.

We may also note that Clune and Green³¹ have made specific-heat measurements in dilute alloys of both Bi and Tl in lead. They find good agreement with rigid-band predictions when they include changes in the phonon enhancement factor with alloying. However, the rate of change of γ with impurity concentration found by Clune and Green is smaller by roughly a factor of 50 than the values obtained by Chol. Their specific-heat results may be more reliable because the superconducting transition is not very sharp in these alloys.

We think that it is not necessary to abandon the RBM. However, the question of whether the fourth zone begins above or below the Fermi energy is not answered clearly by these various results. Although Chol's results indicate that it begins below, not too much weight can be attached to this conclusion because of the disagreement with the measurements of Clune and Green. Our results are not sufficiently accurate to give a clear answer, but because of the good agreement with the RBM at small concentrations, we believe the fourth zone lies above the Fermi energy. Anderson *et al.*²⁷ obtain two models from their fit to the FS; in one the fourth zone lies just above the Fermi energy and in the other it lies just below. The first model with the fourth zone lying above the Fermi energy is favored because of better agreement with pressure dHvA measurements.²⁷ Tobin *et al.*³² have seen low frequency deHaas-Shubnikov oscillations in lead which might be attributed to fourth-zone electrons. These results are somewhat open to question, because they found these low-frequency oscillations very difficult to see (observable only above 80 kOe), indicating a large mass, which one would not expect near the bottom of the fourth zone. Although our results are probably not sensitive enough to detect the actual start of the fourth zone, if they are taken at face value, they would indicate that it begins about 4 meV above the Fermi energy.

It is interesting in passing to determine the effective scattering cross section σ of a bismuth impurity in lead. Classically, the cross section is given by

$$\sigma = 1/Nv\tau, \quad (13)$$

where N is the density of scatterers, v is the electron velocity, and τ is the mean collision time. N is just the concentration C times the atomic density of lead N_0 , and τ is related to the Dingle temperature by $X = \hbar/2\pi k\tau$; we take the velocity to be that calculated

from the Fermi energy of the AG model and the effective mass of Phillips and Gold.²⁵ Then we obtain

$$\sigma = (2\pi k/\hbar N_0 v)(X/C). \quad (14)$$

From our comparison of Dingle temperature with bismuth concentration, $X/C \simeq 674$, neglecting the constant in Eq. (12). Then $\sigma = 0.04a^2$. This value is comparable to the square of the screening length in lead, which is about $0.02a^2$.

One can also obtain a dHvA mean free path $l_D = v\tau$. In the pure material we find a value of $l_D = 3.5 \times 10^4 a$, and in a 0.1% alloy it is $l_D = 5.6 \times 10^3 a$. We note that the average distance between impurities in the 0.1% alloy is much shorter, about $4a$. It is also of interest to compare with values of mean free path obtained from resistivity measurements. Aleksandrov and D'Yakov³³ determined that the temperature dependence of the resistivity of pure lead could be described by the relation

$$\rho T/\rho_{293} = 1.9 \times 10^{-5} + 3.25 \times 10^{-8} T^5. \quad (15)$$

The first term is the residual resistance due to impurity and defect scattering, and the second term has the T^5 dependence expected of the phonon contribution. At 1°K, this expression gives agreement with the resistivity measurements of Phillips and Gold,²⁵ who found a Dingle temperature in good agreement with ours; therefore we believe the above result to be applicable to our samples. It is possible to express the mean free path for resistivity l_p by the following relation (cf. Ziman³⁴):

$$l_p \simeq 12\pi^3 \hbar / e^2 S_F \rho, \quad (16)$$

where S_F is the area of the FS. The AG model of the lead FS gives $S_F = 18.75 \times 10^{16} \text{ cm}^{-2}$, so that one has $l_p = 3.1 \times 10^5 a$ for pure lead at 1.3°K, the temperature at which our measurements were made. Note that $l_D/l_p < 1$, as one might expect, since the dHvA effect is more sensitive to small-angle scattering than the resistivity. Also, the Aleksandrov-D'Yakov result [Eq. (15)] implies that there is no significant contribution to the resistivity from the phonons at 1.3°K, whereas at 4°K the contributions from the two terms are comparable.

CONCLUSIONS

In this study, we have made highly accurate (~ 2 parts in 10^4) measurements of several dHvA frequencies in pure lead, and have observed the variation of the [100] β frequency with the addition of small amounts of bismuth impurity. The pure-lead results represent a refinement of the earlier measurements of AG and are in full agreement with their corrected values.²⁷ The alloy measurements conclusively identify the β oscillations as being due to an electronlike piece of FS, and we therefore concur with AG and Anderson *et al.*⁶ in assigning them to the ν orbit (see Fig. 1).

At small concentrations the dependence of the frequency on concentration is in good agreement with the predictions of the RBM. At the larger concentrations there is a tendency for the frequency changes to fall below the RBM predictions, and we interpret this trend to be due to an increase in the density of states, indicating that electrons are beginning to fill the fourth zone. This result is consistent with the superconducting critical field work of Chol¹⁷ and Pech.¹⁶ There remains some ambiguity as to whether the fourth zone actually begins above or below the Fermi energy, but our results, taken at face value, would lead us to suggest that it begins ~ 4 meV above the pure-lead Fermi energy.

The technique of using *in situ* NMR to measure field is primarily responsible for the accuracy of the

pure-lead measurements and for the sensitivity obtained, which is required to measure the small changes in the FS in the alloys. The present accuracy is greater than can be utilized by most band calculations, and it compares favorably with the relative accuracy attainable in dHvA rotation diagrams. In short, the *in situ* NMR technique appears to be a powerful tool for the investigation of small absolute changes in the FS of metals.

ACKNOWLEDGMENTS

We are especially indebted to Dr. D. R. Stone for many helpful conversations. The support of the University of Maryland Computer Science Center is gratefully acknowledged.

* Work supported by the Advanced Research Projects Agency. Parts of this paper are based upon a thesis submitted by Dr. Hines in partial fulfillment of the requirements for a Ph.D. in Physics, University of Maryland, College Park, Md.

† Present address: Lockheed Missiles and Space Co., Bldg. 151, Dept. 62-31, P.O. Box 504, Sunnyvale, Calif. 94088.

¹ W. Hume-Rothery, *The Metallic State* (Oxford U. P., London, 1936), p. 328.

² J. P. G. Shepherd and W. L. Gordon, *Phys. Rev.* **169**, 541 (1968).

³ A. V. Gold, *Phil. Trans.* **A251**, 85 (1958).

⁴ R. J. Higgins and J. A. Marcus, *Phys. Rev.* **141**, 553 (1966).

⁵ J. R. Anderson and A. V. Gold, *Phys. Rev.* **139**, A1459 (1965).

⁶ J. R. Anderson, W. J. O'Sullivan, and J. E. Schirber, *Phys. Rev.* **153**, 721 (1967).

⁷ I. M. Lifshitz and A. M. Kosevich, *Zh. Eksperim. i Teor. Fiz.* **29**, 730 (1955) [*Soviet Phys. JETP* **2**, 636 (1956)].

⁸ R. B. Dingle, *Proc. Roy. Soc. (London)* **A211**, 517 (1952).

⁹ A. D. Brailsford, *Phys. Rev.* **149**, 456 (1966).

¹⁰ C. Tyzack and G. V. Raynor, *Acta Cryst.* **7**, 505 (1954).

¹¹ V. Heine, *Proc. Phys. Soc. (London)* **A69**, 505 (1956).

¹² N. F. Mott, *Proc. Cambridge Phil. Soc.* **32**, 281 (1936).

¹³ J. Friedel, *Advan. Phys.* **3**, 446 (1954).

¹⁴ R. J. Higgins, H. D. Kaehn, and J. H. Condon, *Phys. Rev.* **181**, 1059 (1969).

¹⁵ W. J. O'Sullivan, A. C. Switendick, and J. E. Schirber, *Natl. Bur. Std. (U.S.) Spec. Publ.* **323** (1970).

¹⁶ M. Pech, *J. Phys. Radium* **23**, 591 (1962).

¹⁷ P. G. Chol, *J. Phys. Radium* **25**, 374 (1964).

¹⁸ M. Cutler, *Phys. Rev.* **181**, 1102 (1969).

¹⁹ J. Vanderkooy, J. S. Moss, and W. R. Datars, *J. Sci. Instr.* **44**, 949 (1967).

²⁰ D. Shoenberg and P. J. Stiles, *Proc. Roy. Soc. (London)* **A281**, 62 (1964).

²¹ R. W. Stark, L. R. Windmiller, and J. B. Ketterson, *Cryogenics* **8**, 272 (1968).

²² D. C. Hines, Ph.D. thesis, University of Maryland, 1970 (unpublished).

²³ D. A. Hill and C. Hwang, *J. Sci. Instr.* **43**, 581 (1966).

²⁴ W. D. Knight, in *Solid State Physics* edited by F. Seitz and D. Turnbull (Academic, New York, 1956), Vol. 2, p. 130.

²⁵ R. A. Phillips and A. V. Gold, *Phys. Rev.* **178**, 932 (1969).

²⁶ Ledoux and Co., 359 Alfred Ave., Teaneck, N.J. 07666.

²⁷ J. R. Anderson, W. J. O'Sullivan, and J. E. Schirber (unpublished).

²⁸ W. J. O'Sullivan and J. E. Schirber, *Cryogenics* **7**, 118 (1967).

²⁹ B. J. C. van der Hoeven and P. H. Keesom, *Phys. Rev.* **137**, A103 (1965).

³⁰ S. T. Sekula and R. H. Kernohan, *J. Phys. Chem. Solids* **27**, 1863 (1966).

³¹ Lavern C. Clune and Ben A. Green, Jr., *Phys. Rev. B* **1**, 1459 (1970).

³² P. J. Tobin, D. J. Sellmyer, and B. L. Averbach, *Phys. Letters* **28A**, 723 (1969).

³³ B. N. Aleksandrov and I. G. D'Yakov, *Zh. Eksperim. i Teor. Fiz.* **43**, 852 (1962) [*Soviet Phys. JETP* **16**, 603 (1963)].

³⁴ J. M. Ziman, *Principles of the Theory of Solids* (Cambridge U. P., Cambridge, England, 1965), p. 183.

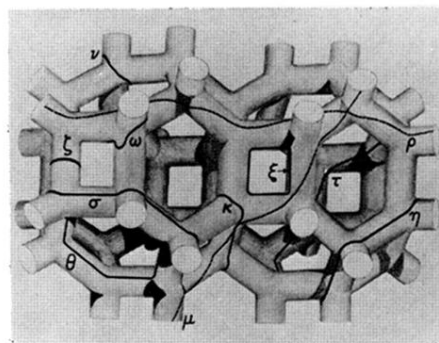


FIG. 1. Third-zone Fermi surface of lead (schematic).